PHYSICAL REVIEW E **79**, 045303(R) (2009)

Effect of nonharmonic forcing on bluff-body vortex dynamics

E. Konstantinidis* and D. Bouris†
Department of Engineering and Management of Energy Resources, University of Western Macedonia, Kozani 50100, Greece
(Received 21 January 2009; published 15 April 2009)

Forced nonharmonic excitation of the two-dimensional flow about a circular cylinder is studied by numerical simulations at mean Reynolds numbers of 180 and 150. Moderate deviations of the forced inflow velocity waveform from a pure harmonic generate different modes of phase-locked vortex formation in the cylinder wake, involving combinations of single and/or pairs of vortices for the same forcing frequency and peak-to-peak amplitude. The dynamical response of the wake oscillator is studied by employing phase portraits of the drag and lift coefficients that display modified limit-cycle behavior due to nonharmonic excitation. It is further shown that changing solely the velocity waveform can incite transition from a quasiperiodic state to a phase-locked state. The findings demonstrate that the wake oscillator is admissible to an infinite number of phase-locked and/or modulated states characterized by a single point on the frequency-amplitude plane.

DOI: 10.1103/PhysRevE.79.045303 PACS number(s): 47.32.ck, 47.20.Pc

The flow in the wake of a bluff body behaves as a self-excited fluid oscillator above a critical Reynolds number. The onset of global wake oscillations occurs through a Hopf bifurcation as explained from hydrodynamic stability theory [1]. In the observation domain, this instability is manifested by the formation of a spatiotemporal flow pattern well known as the Kármán vortex street. Beyond the critical point further instabilities lead progressively to three dimensionality and turbulence in the wake as a function of the Reynolds number [2]. The vorticity dynamics in the near wake play an essential role in determining the frequency of the primary instability in the absence of external perturbations [3]. From the dynamical systems point of view, when the fluid oscillator is externally forced, it is possible to attain wake states that are strictly periodic or phase locked, quasiperiodic or modulated, and/or chaotic in general [4,5]. The wake flow can be thought of as a nonlinear oscillator whose limit-cycle behavior is modified by forcing generating a rich variety of orbits in phase space. Such a response is commensurate to the modes of vortex formation in bluff-body wakes that have been observed in numerous studies where the Kármán mode is perturbed by rectilinear or rotational oscillations of the body, inflow pulsations, sound waves, and other types of excitation, e.g., see Refs. [6–9]. The dynamical response of the wake oscillator to any forced excitation displays notable similarities as a function of the forcing frequency and amplitude, parameters which define completely the waveform for harmonic drivers, along with the Reynolds number which acts as an intrinsic excitation. Coupling effects are most visible in an envelope on the frequency-amplitude plane around the intrinsic frequency of the flow instability in the absence of forcing where phase locking occurs (alias the lock-on range). Within this range, the modes and phasing of vortex formation, the fluid-dynamic forces on the cylinder and the time-averaged properties of the flow can be controlled within limits by the forced excitation. Hence, the forcing frequency and amplitude provide a means for optimization of the flow parameters to a given task, e.g., drag reduction, mixing enhancement, flow destabilization, control, etc. An important aspect of the present work is that new control possibilities exist by adjusting the waveform of the forcing drivers.

The fluid dynamics of bluff cylinders in forced harmonic oscillation have traditionally been employed to study and model interactions occurring in coupled fluid-mechanical oscillators, e.g., the vortex-induced vibration of hydroelastic cylinders [10,11]. The use of harmonic forcing poses a limitation on the spectrum of response characteristics and associated energy transfer between the fluid and the cylinder since the actual vibration is seldom a pure harmonic oscillation. Therefore, it seems rational to examine nonharmonic periodic functions as forcing terms and address their effect on the system dynamics. For example, nonharmonic forcing has been previously employed to switch the response of a nonlinear parametric pendulum [12]. Such a forcing has a well-defined periodic waveform which comprises an infinite number of harmonics; to our knowledge there are no similar studies of nonharmonic forcing in spatially extended systems as is the wake of a bluff body.

In this work, we show that the modes of vortex formation in the wake of a circular cylinder and the fluid loading on the cylinder are sensitive to nonharmonic forcing even for drivers of the same period and amplitude. This study is limited to laminar and two-dimensional (2D) cylinder wakes for which the response to external forcing is deterministic in the absence of stochastic perturbations [13]. Although 2D simulations inherently hold a simplifying assumption compared to three-dimensional (3D) approaches, it is expected that for the parameters employed in this study the physics of shear layer separation and eventual vortex formation in the near wake remain laminar and two dimensional. The continuity and Navier-Stokes equations for an incompressible fluid were solved numerically on an orthogonal curvilinear mesh with sufficient resolution (299×208) to produce mesh-independent results. The code is based on the SIMPLE algorithm employing first-order implicit Euler discretization for integration in time, while for the spatial discretization a second-order bounded upwind scheme and central differencing were employed for the convection and diffusion terms, respectively. Further details of the numerical method can be found in Ref. [14]. The computational domain is rectangular, 34 dimensionless units long and 20 wide which is large

*ekonstantinidis@uowm.gr
†dmpouris@uowm.gr

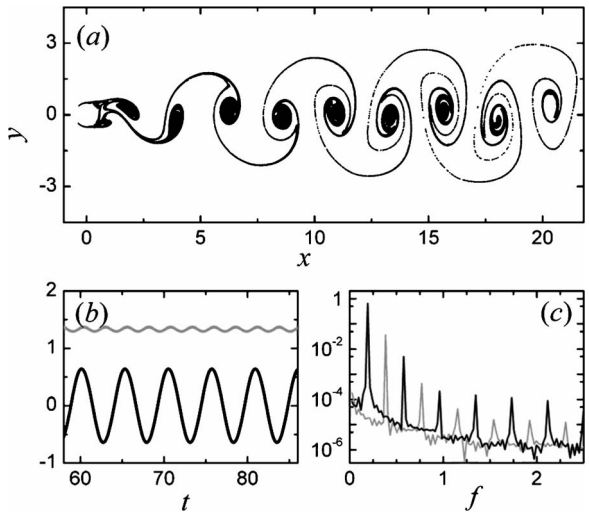

FIG. 1. Characteristics of the natural cylinder wake in the absence of forcing at $Re=180$. (a) Particle visualization of the wake, (b) time history of the force coefficients, and (c) magnitude spectra of the force coefficients. Grey and black lines in (b) and (c) correspond to the drag and lift coefficients, respectively.

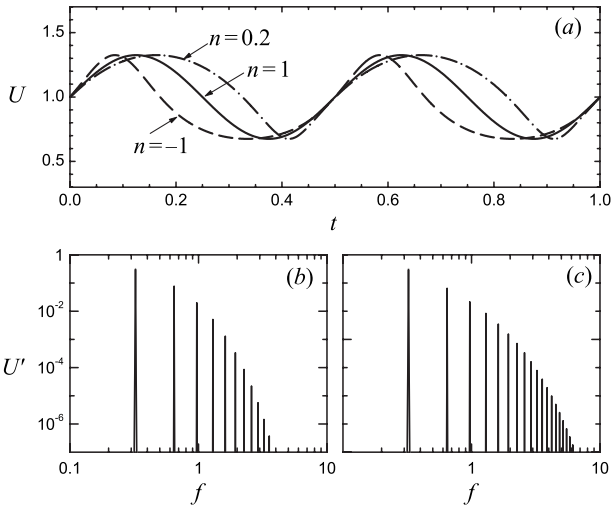

FIG. 2. (a) Plot of some velocity waveforms $U(t)$ with equal period and peak-to-peak amplitude used to perturb the inflow. Frequency content of the fluctuating part U' of the nonharmonic velocity waveforms; (b) $n=0.2$ and (c) $n=-1$.

enough to produce results independent of the location of the boundaries [15]. At the inflow boundary of the computational domain a time-dependent velocity waveform is prescribed in order to act as an excitation source. A no-slip condition is imposed on the cylinder surface, symmetry conditions are employed at the lateral boundaries, whereas at the outflow boundary a free-convection condition is employed. In the presentation of the results the variables are normalized using the diameter of the cylinder and the reference velocity.

Figure 1(a) shows vortex formation in the natural wake without forcing. The Kármán vortex street consisting of an alternating row of oppositely rotating vortices is well reproduced by the simulation. The fluctuating drag and lift forces exerted on the cylinder due to vortex shedding and their magnitude spectra are shown in Figs. 1(b) and 1(c), respectively. The computed values of the mean drag coefficient ($C_D=1.33$) and of the fluctuating lift coefficient ($C_L'=0.643$) are consistent with other published data [16]. The lift and drag spectra exhibit a dominant peak at the Strouhal frequency $f_{St}=0.192$ and its first superharmonic, respectively. It is observed that both components contain an infinite number of superharmonics of the main frequency with substantially lower but finite magnitude. This salient observation indicates that the self-excited wake flow is indeed a nonlinear oscillator, and it might be anticipated that nonharmonic excitation containing an infinite number of harmonics can interact with the bluff-body vortex dynamics in a different way compared to pure harmonic excitation, as subsequently shown.

Forced excitation was invoked by a velocity perturbation in the inflow boundary using waveforms $U(t)$ generated by the following function:

$$U(t) = [1 + \alpha \sin^2(\omega t + \phi)]^n + \beta, \tag{1}$$

where ω is the cyclic frequency of forcing, α, β, and n, are parameters that control the amplitude of the velocity perturbation, the average flow velocity, and the waveform of the drivers, respectively. The period and the profile of the waveforms generated by Eq. (1) are independent of α and β. A phase shift ϕ was employed so that the velocity at zero time is also equal to the average of the minimum and maximum velocities in the waveform $U_0=\frac{1}{2}(U_{max}+U_{min})=1$ in all cases. In this way, the same flow field at the end of the run without forcing could be used as an initial field for all the simulations of forced wakes. For $n=1$, a pure harmonic excitation at twice the nominal forcing frequency is obtained. Harmonic forcing provides here the basis for comparisons of the wake response. Figure 2 shows the nonharmonic waveforms for $n=0.2$ and -1 together with the harmonic one ($n=1$) employed in the present study. The other two variables, α and β, were adjusted so that the minimum and maximum velocities remain the same as in the pure harmonic to allow comparisons between different waveforms. The frequency content of the nonharmonic velocity waveforms is also shown in Fig. 2. The spectral peak at the main forcing frequency in both nonharmonic velocity waveforms is indistinguishable from that in the pure harmonic and contains more than 93.5% of the total kinetic energy, i.e., the deviation from the harmonic waveform can be characterized as moderate.

Initially, we present results for simulated flows with purely harmonic and nonharmonic forcing at $Re=180$ based on the reference velocity at zero time U_0, the cylinder diameter, and the fluid kinematic viscosity. The ratio of the forcing frequency to that of natural vortex shedding in the unforced wake f_{St} was set to $\Omega=0.84$. The other variables α and β were adjusted so that the maximum and minimum velocities are 1 ± 0.325, respectively. The parameter $\epsilon=\max|U(t)-U_0|=0.325$ defines the dimensionless amplitude of forced excitation and provides a measure of the nonlinear coupling between the forced and self-excitation modes.

Figure 3 provides some representative results from the

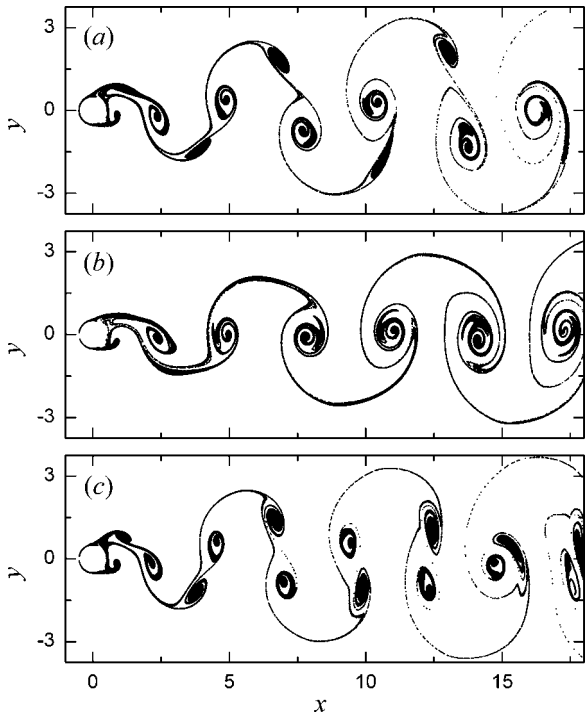

FIG. 3. Modes of vortex formation in forced cylinder wakes for harmonic and nonharmonic excitation waveforms; (a) $n=1$, (b) $n=0.2$, and (c) $n=-1$

simulations by means of particle visualization [17]. For purely harmonic forcing ($n=1$), an asymmetric pattern with respect to the centerline is observed; the vortex street comprises a combination of single, and pairs of vortices shed from alternate sides of the cylinder. Closer examination shows that a vortex pair is actually formed on either side. However, the secondary vortex from the lower side is absorbed by the initial vortex shed from the same side. On the other (upper) side, the shed vortices maintain their integrity as they are convected downstream. This asymmetric mode of vortex formation has been consistently observed in a number of studies, both numerical and experimental, dealing with forced wakes [6,18–21]. Nonharmonic excitation may promote the formation of either distinct individual or pairs of vortices depending on the velocity waveform as shown in Fig. 3. For $n=0.2$, the secondary vortices almost disappear and the ensuing vortex street comprises a row of alternating single vortices with opposite sense of rotation similar to that observed in the natural wake. However, in the forced wake the vortices from the upper side are convected below the centerline after being shed, and vice versa. Another difference is that the longitudinal spacing between vortices is expanded in the forced wake since the period of vortex formation is prolonged. For $n=-1$, distinct vortex pairs are formed on both sides; the initial vortices are less pronounced than the secondary ones as indicated by the concentration of tracer particles in the vortex cores. This mode of vortex formation leads to an unstable vortex street and vortices with the same sense of rotation tend to coalesce further downstream, e.g., ten diameters from the cylinder. Effectively, this is a 2D numerical simulation that captures the shedding of vortex pairs in forced laminar bluff-body wakes.

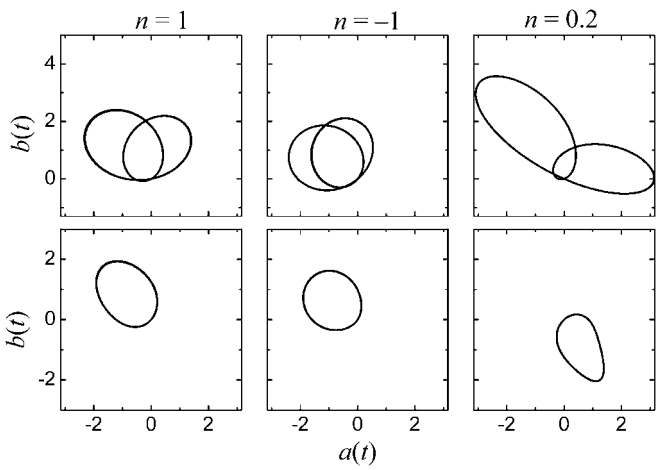

FIG. 4. Phase portraits of the fluctuating drag (upper row) and lift coefficients (lower row) for different velocity waveforms.

The temporal dynamics of the forced cylinder wakes is characterized by the phase portraits of the fluctuating drag $C_D(t)$ and lift $C_L(t)$ coefficients shown in Fig. 4. The abscissa $a(t)$ and the ordinate $b(t)$ in the plots were computed from the instantaneous force coefficients as

$$a(t) = C_D'(t)\sin(2\omega t), \quad b(t) = C_D'(t)\cos(2\omega t) \tag{2}$$

for the drag component, and

$$a(t) = C_L'(t)\sin(\omega t), \quad b(t) = C_L'(t)\cos(\omega t) \tag{3}$$

for the lift component, where the primes denote the fluctuating part only (mean value subtracted), and the instantaneous velocity was used for the normalization of the forces. Such plots provide information on the instantaneous magnitude, $(a^2+b^2)^{1/2}$, and the phase angle, $\arctan(b/a)$, of time-dependent signals with respect to forcing [22]. We employ the analysis on the drag and lift signals because they represent the integrated effect of the vortex dynamics and illustrate its modification by nonharmonic forcing.

The response of the drag coefficient, though phase locked with the forcing (limit cycle), is far from a circular orbit (i.e., harmonic) for both harmonic and nonharmonic excitations. In fact, the phase portrait of $C_D(t)$ follows a different orbit for even and odd cycles, illustrating the effect of the asymmetric mode of vortex formation under harmonic forcing which persists even when no identifiable asymmetry is observed in the wake structure under nonharmonic forcing. Interestingly, the phase portrait of $C_L(t)$ displays a limit-cycle behavior without any notable deviation between even and odd cycles of forced excitation. However, it is observed that the final periodic state for $n=0.2$ is shifted by half a period, i.e., vortices are shed from opposite sides of the cylinder for even and odd cycles compared to the other two cases. Unlike $C_D(t)$, the lift component is not directly affected by the forcing which acts only in the flow direction and the modified limit cycles of $C_L(t)$ can be solely attributed to the changes in the vortex dynamics around the body.

A survey of computations was carried out on the frequency-amplitude $\{\Omega, \epsilon\}$ plane near the boundaries of the

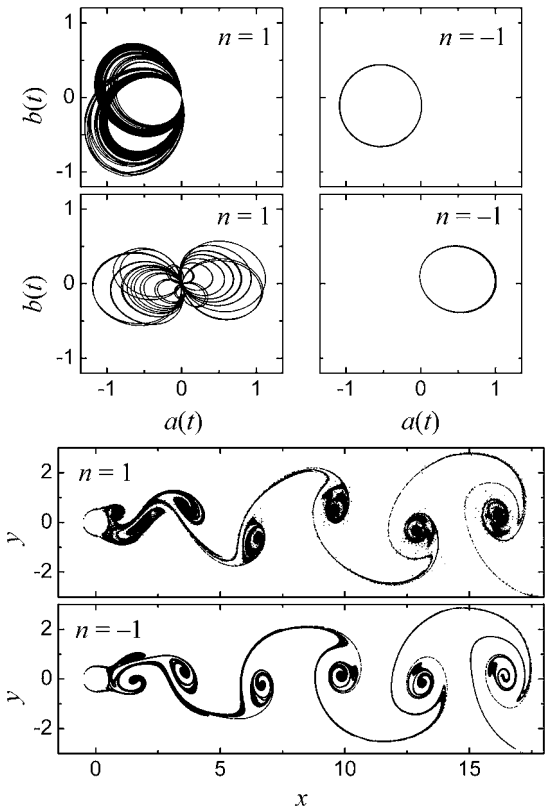

FIG. 5. Phase portraits of $C_D'(t)$ in the first row and $C_L'(t)$ in the second row for two different velocity waveforms, $n=-1$ and 1, and the corresponding modes of vortex formation in the wake, below. Forced excitation: $Re=150$, $\Omega=0.75$, and $\epsilon=0.20$.

lock-on envelope where transition between lock-on and non-lock-on responses occurs for harmonic forcing. It was found that changing solely the forcing waveform can incite transition from a quasiperiodic non-lock-on to a phase-locked state as illustrated in Fig. 5. This clearly indicates that the wake oscillator is admissible to different dynamical states corresponding to a single point in the $\{\Omega,\epsilon\}$ plane but different waveforms. Nevertheless, it should be noted that the dynamical states observed in the present study are possibly few out of an infinite number of admissible states in bluff-body wakes. While the corresponding modes of vortex formation are similar for both harmonic and nonharmonic forcings most of the time, Fig. 5 shows an instant where the vortex mode for the harmonic case sporadically deviates from that for nonharmonic excitation.

In conclusion, the importance of the present findings is not simply due to the considerable and new effects that nonharmonic forcing has on bluff-body vortex dynamics; they also have practical implications for the corresponding problem of self-sustained vortex-induced vibration of hydroelastic cylinders. Vortex-induced vibration involves cross excitation of the wake (fluid oscillator) and the cylinder vibration (mechanical oscillator) resulting in a nonlinear dynamical system. In this case, a question arises as to the selection of a dynamical state by such a coupled system. Based on the outcome of the present study it is suggested that coupled fluid-mechanical oscillators, where the response variables (i.e., the frequency and amplitude of oscillation) are determined by nonlinear interactions and energy balances, can be characterized by a *continuously modulated periodic state around an equilibrium point* on the frequency-amplitude plane. In other words, a hydroelastic cylinder can continuously adapt its dynamics to an infinite number of admissible states so as to exhibit self-sustained oscillations. This scenario can account for the fact that most of the free vibration occurs near the boundaries of the lock-on envelope or even where forced harmonic vibration studies indicate lack of lock on [23]. Similar effects are visible when a mechanical oscillator with two degrees of freedom conspires with the vortex dynamics in turbulent wakes to cause even stronger nonharmonic perturbations which lead to the shedding of vortex triplets [24].

[1] G. S. Triantafyllou, K. Kupfer, and A. Bers, Phys. Rev. Lett. **59**, 1914 (1987).
[2] C. H. K. Williamson, Annu. Rev. Fluid Mech. **28**, 477 (1996).
[3] F. L. Ponta and H. Aref, Phys. Rev. Lett. **93**, 084501 (2004).
[4] G. E. Karniadakis and G. S. Triantafyllou, J. Fluid Mech. **199**, 441 (1989).
[5] D. J. Olinger and K. R. Sreenivasan, Phys. Rev. Lett. **60**, 797 (1988).
[6] C. H. K. Williamson and A. Roshko, J. Fluids Struct. **2**, 355 (1988).
[7] O. M. Griffin and H. S. Hall, J. Fluids Eng. **113**, 526 (1991).
[8] M. M. Zdravkovich, J. Fluids Struct. **10**, 427 (1996).
[9] E. Konstantinidis, S. Balabani, and M. Yianneskis, Phys. Fluids **19**, 011701 (2007).
[10] P. W. Bearman, Annu. Rev. Fluid Mech. **16**, 195 (1984).
[11] T. Sarpkaya, J. Fluids Struct. **19**, 389 (2004).
[12] M. A. F. Sanjuán, Phys. Rev. E **58**, 4377 (1998).
[13] D. Lucor and G. E. Karniadakis, Phys. Rev. Lett. **92**, 154501 (2004).
[14] D. Bouris, E. Konstantinidis, S. Balabani, D. Castiglia, and G. Bergeles, Int. J. Heat Mass Transfer **48**, 3817 (2005).
[15] M. Behr, D. Hastreiter, S. Mittal, and T. E. Tezduyar, Comput. Methods Appl. Mech. Eng. **123**, 309 (1995).
[16] R. D. Henderson, Phys. Fluids **7**, 2102 (1995).
[17] See EPAPS Document No. E-PLEEE8-79-R05904 for particle visualization animations. For more information on EPAPS, see http://www.aip.org/pubservs/epaps.html.
[18] A. Ongoren and D. Rockwell, J. Fluid Mech. **191**, 225 (1988).
[19] J. R. Meneghini and P. W. Bearman, J. Fluids Struct. **9**, 435 (1995).
[20] H. M. Blackburn and R. D. Henderson, J. Fluid Mech. **385**, 255 (1999).
[21] J. S. Leontini, B. E. Stewart, M. C. Thompson, and K. Hourigan, Phys. Fluids **18**, 067101 (2006).
[22] S. J. Baek and H. J. Sung, J. Fluid Mech. **408**, 275 (2000).
[23] T. K. Prasanth and S. Mittal, J. Fluid Mech. **594**, 463 (2008).
[24] J. M. Dahl, F. S. Hover, M. S. Triantafyllou, S. Dong, and G. E. Karniadakis, Phys. Rev. Lett. **99**, 144503 (2007).